ISSN 1064-5624, Doklady Mathematics, 2018, Vol. 98, No. 2, pp. 506–510. © Pleiades Publishing, Ltd., 2018.
Original Russian Text © N.A. Zyuzina, O.A. Kovyrkina, V.V. Ostapenko, 2018, published in Doklady Akademii Nauk, 2018, Vol. 482, No. 6.

MATHEMATICS

Monotone Finite-Difference Scheme Preserving High Accuracy in Regions of Shock Influence

N. A. Zyuzina[a,b], O. A. Kovyrkina[a], and V. V. Ostapenko [a,*]

Presented by Academician of the RAS B.N. Chetverushkin May 3, 2018

Received May 31, 2018

Abstract—An explicit combined shock-capturing finite-difference scheme is constructed that localizes shock fronts with high accuracy and simultaneously preserves the high order of convergence in all domains where the computed weak solutions are smooth. In this scheme, Rusanov's explicit nonmonotone scheme of the third order is used as a basis one, while the internal scheme is based on the second-order monotone CABARET. The advantages of the new scheme as compared with the WENO scheme of the fifth order in space and third order in time are demonstrated in test computations.

DOI: 10.1134/S1064562418060315

1. In his classical work [1] associated with a solution technique for Riemann problems, Godunov introduced the concept of a monotone finite-difference scheme and proved that, among linear difference schemes, there are no monotone ones with an order of accuracy higher than the first. The subsequent development of the theory of shock-capturing difference schemes for hyperbolic systems of conservation laws was aimed to a large degree at the overcoming of the Godunov order barrier. As a result, various classes of difference schemes were developed in which a high order of accuracy for smooth solutions and monotonicity were achieved by applying nonlinear flux correction (NFC), which leads to the nonlinearity of these schemes even in the approximation of the linear transport equation. The basic classes of NFC schemes include MUSCL [2], TVD [3], NED [4], WENO [5], and CABARET [6] schemes. The basic advantage of these schemes is that they localize shock waves with high accuracy in the absence of considerable spurious oscillations on their fronts.

It has been shown that NFC schemes have at most the first order of both local convergence in shock influence regions [7–9] and integral convergence on intervals with one of the boundaries lying in a shock influence region [10–12]. The cause of this is that the flux correction procedure characteristic of NFC schemes leads to less smooth numerical fluxes, which in turn lead to a lower order of approximation of the Hugoniot ε-conditions on shock fronts [13]. At the same time, classical high-order accurate nonmonotone schemes that have analytical functions of numerical fluxes and, hence, approximate the Hugoniot ε-conditions with high accuracy preserve the high order of convergence in negative norm in integration over domains containing strong discontinuities [10, 11]. As a result, these nonmonotone schemes, in contrast to NFC ones, preserve the high order of convergence in regions of shock influence despite the noticeable spurious oscillations on their fronts.

In [14], a method was proposed for constructing shock-capturing difference schemes that combine the advantages of both NFC and classical nonmonotone schemes, namely, they localize shock fronts with high accuracy and simultaneously preserve the high order of convergence in all domains where the considered weak solutions are smooth. A combined difference scheme involves a nonmonotone basis scheme of high order of convergence applied in regions of shock influence. The basis scheme is used to construct a difference solution in the entire computational domain. In high-gradient regions, where this solution has spurious oscillations, it is corrected by solving internal initial–boundary value problems with the help of an NFC scheme. In the combined scheme considered in [14], a compact scheme of the third order of weak approximation was used as a basis one [10] and the internal NFC scheme was the CABARET one, which is second-order accurate for smooth solutions [6].

The basic disadvantage of the combined scheme constructed in [14] is that the corresponding basis and internal schemes have widely different types: the basis

[a] *Lavrent'ev Institute of Hydrodynamics, Siberian Branch, Russian Academy of Sciences, Novosibirsk, 630090 Russia*
[b] *Novosibirsk State University, Novosibirsk, 630090 Russia*
**e-mail: ostapenko_vv@ngs.ru*

compact scheme is implicit and three-time-level, while the internal CABARET scheme is explicit and two-time-level. As a result, difficulties arise in the numerical implementation of such an algorithm. Accordingly, we propose a new combined finite-difference scheme in which the nonmonotone basis one and the internal NFC one are both explicit and have two levels in time. More specifically, Rusanov's third-order scheme [15] and a monotone second-order modification of the CABARET scheme are used as basis and internal ones. The advantages of the new scheme as compared with the WENO scheme of the fifth order in space and the third order in time [5] are demonstrated using test computations.

2. Consider a quasilinear hyperbolic system of conservation laws

$$\mathbf{u}_t + \mathbf{f}(\mathbf{u})_x = 0, \tag{1}$$

where $\mathbf{u}(x,t)$ and $\mathbf{f}(\mathbf{u})$ are the unknown and given smooth vector functions, respectively, containing k components. For system (1), we set up the Cauchy problem with smooth periodic initial data

$$\mathbf{u}(x,0) = \mathbf{v}(x) \equiv \mathbf{v}(x+X). \tag{2}$$

Assume that problem (1), (2) has a unique weak solution $\mathbf{u}(x,t)$ that contains a shock wave on an interval of period length X arising due to a gradient catastrophe at some time $T_0 > 0$. A combined finite-difference scheme approximating this problem is constructed on a rectangular grid

$$S = \{(x_j,t_n): x_j = j\Delta, 0 \le j \le N; t_{n+1} = t_n + \tau_n, t_0 = 0\}, \tag{3}$$

where $\Delta = \dfrac{X}{N}$ is the (constant) mesh size in space,

$$\tau_n = \frac{z\Delta}{\max\limits_{k,j} |a_k(\mathbf{u}_j^n)|}$$

is the time step determined by the Courant condition with $a_k(\mathbf{u})$ being the eigenvalues of the Jacobian matrix $\mathbf{f}_\mathbf{u}$ of system (1), and $z = 0.5$ is the safety factor.

Test computations have shown that oscillations arising on shock waves in classical nonmonotone schemes of high accuracy carry information on the wave structure of the Fourier series expansion of the strong discontinuity at the shock front; as a result, these schemes approximate the Hugoniot ε-conditions on shock waves with high accuracy. In NFC schemes (which suppress oscillations on shock waves), this information is lost, which leads to their reduced accuracy in regions of shock influence. Therefore, in the combined scheme, the periodic difference solution

$$\mathbf{u}_j^n = \mathbf{u}(x_j,t_n) \equiv \mathbf{u}(x_{j+N},t_n)$$

of Cauchy problem (1), (2) produced by Rusanov's scheme is independent of the difference solution $\mathbf{v}_j^n = \mathbf{v}(x_j,t_n)$ based on the internal CABARET scheme, which is used to smooth oscillations in the grid neighborhood

$$\begin{aligned} S_c = \{(x_j,t_n): j_n - m \le j \le j_n + m + 1,\\ |\tilde{\mathbf{u}}_{j_n+1/2}^n| = \max_j |\tilde{\mathbf{u}}_{j+1/2}^n| \ge p\} \end{aligned} \tag{4}$$

of the smeared shock front, where $m > 0$ is an integer specifying the width of the domain S_c, $\tilde{\mathbf{u}}_{j+1/2}^n = \dfrac{\mathbf{u}_{j+1}^n - \mathbf{u}_j^n}{\Delta}$ is the spatial difference derivative, and $p \ge 1$ is a parameter determining the beginning of the formation of a numerical shock wave.

The monotone difference solution $\mathbf{v}_j^n$ is obtained by solving the initial–boundary value problem for system (1) in domain (4) by applying the monotone modification of the CABARET scheme. The initial and boundary conditions for this interior problem are specified using the difference solution $\mathbf{u}_j^n$ produced by Rusanov's scheme. As a result, the combined difference scheme yields the solution

$$\mathbf{w}_j^n = \begin{cases} \mathbf{u}_j^n, & (x_j,t_n) \in S \backslash S_c, \\ \mathbf{v}_j^n, & (x_j,t_n) \in S_c. \end{cases} \tag{5}$$

The basic advantage of this solution is that it preserves high accuracy in the region of shock influence (due to Rusanov's third-order scheme used in the entire computational domain) and simultaneously monotonically localizes the shock wave (due to the second-order monotone modification of the CABARET scheme applied in a neighborhood of its front).

The technique described allows yields the smoothed solution $\mathbf{v}_j^n$ in domain (4) after the basis solution $\mathbf{u}_j^n$ was obtained in the entire computational domain (3). However, in practice, it is more convenient to find these solutions simultaneously at each time level. Given the solutions $\mathbf{u}_j^n$ and $\mathbf{v}_j^n$ and, hence, the solution $\mathbf{w}_j^n$ at the nth time level, Rusanov's basis scheme is first used to find the solution $\mathbf{u}_j^{n+1}$ at the $(n+1)$th time level of domain (3). This solution specifies the boundary conditions at the spatial nodes $j_{n+1} - m$ and $j_{n+1} + m + 1$, which are used to determine the solution $\mathbf{v}_j^{n+1}$ at the $(n+1)$th time level of domain (4) by applying the internal CABARET scheme. As a result, the solution $\mathbf{w}_j^{n+1}$ of the combined difference scheme at the $(n+1)$th time level of computational domain (3) is given by formula (5).

3. As a particular hyperbolic system, we use the shallow water equations in the first approximation. Written in conservative form in the case of a rectangular horizontal channel without bottom friction, they have the form of (1), where

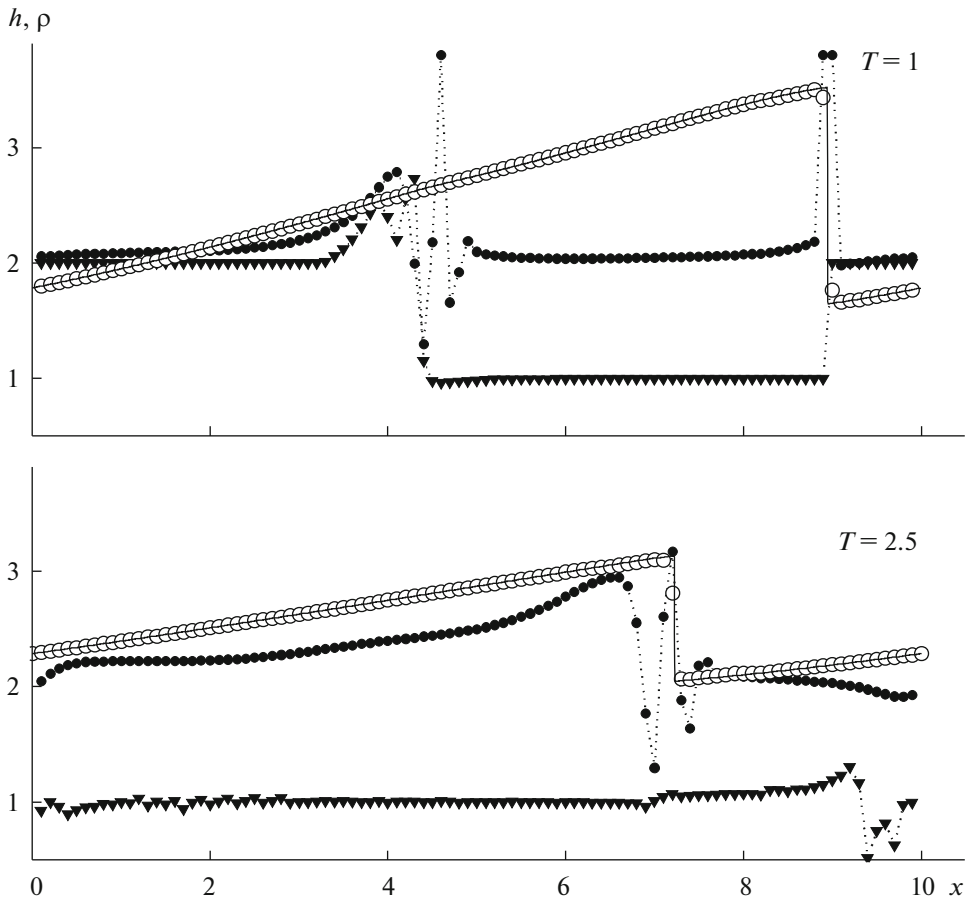

Fig. 1. Fluid depth produced by the combined scheme (open circles) and the integral orders of convergence in Rusanov's scheme (solid circles) and the WENO scheme (triangles). The solid line depicts the exact solution modeled by the CABARET scheme on a fine grid.

$$\mathbf{u} = \begin{pmatrix} h \\ q \end{pmatrix}, \quad \mathbf{f}(\mathbf{u}) = \begin{pmatrix} q \\ \dfrac{q^2}{h} + \dfrac{gh^2}{2} \end{pmatrix}. \tag{6}$$

Here, $h(x,t)$ is the depth of the flow, $q(x,t)$ is the flow rate, and g is the acceleration of gravity (in the computations, $g = 10$). For system (1), (6), we consider Cauchy problem (2) with periodic initial data

$$\begin{aligned} v(x,0) &= a\sin\left(\frac{2\pi x}{X} + \frac{\pi}{4}\right), \\ h(x,0) &= \frac{1}{4g}\left(a\sin\left(\frac{2\pi x}{X} + \frac{\pi}{4}\right) + b\right)^2, \end{aligned} \tag{7}$$

where $v(x,t) = \dfrac{q(x,t)}{h(x,t)}$ is the fluid velocity (this problem was considered in [11, 14]). The initial data (7) correspond to the following initial values of the invariants $w_1 = v - 2c$ and $w_2 = v + 2c$:

$$\begin{aligned} w_1(x,0) &= -b, \\ w_2(x,0) &= 2v(x,0) + b = 2a\sin\left(\frac{2\pi x}{X} + \frac{\pi}{4}\right) + b, \end{aligned}$$

where $c = \sqrt{gh}$, $a = 2$, $b = 10$, and $X = 10$.

The exact solution of this problem is simulated by applying the CABARET scheme on a fine grid with spatial stepsize $\Delta = 0.005$. The depth profiles obtained at the times $T = 1$ and $T = 2.5$ are shown by the solid line in Fig. 1 (on an interval of period length) and in Fig. 2 (near the shock front). The numerical results for the given problem on a grid with the spatial stepsize $\Delta = 0.1$ as obtained using the combined, WENO, and Rusanov's schemes are shown in Figs. 1 and 2. Oscillations arising in Rusanov's scheme near the shock front can be seen in Fig. 2. In the combined scheme, they are smoothed out by applying the CABARET scheme in domain (4), where $m = 6$ and $p = 1$. In the combined scheme, the shock front is smeared considerably less than in the WENO scheme.

For the difference solution on the intervals $[x_j, X]$, in Fig. 1 shows the orders of integral convergence ρ_j obtained in Rusanov's scheme (solid circles) and the WENO scheme (triangles). Figure 3 presents the grid functions $(r_i)_j = \log|\delta w_i(x_j)|$ at the time $T = 2.5$,

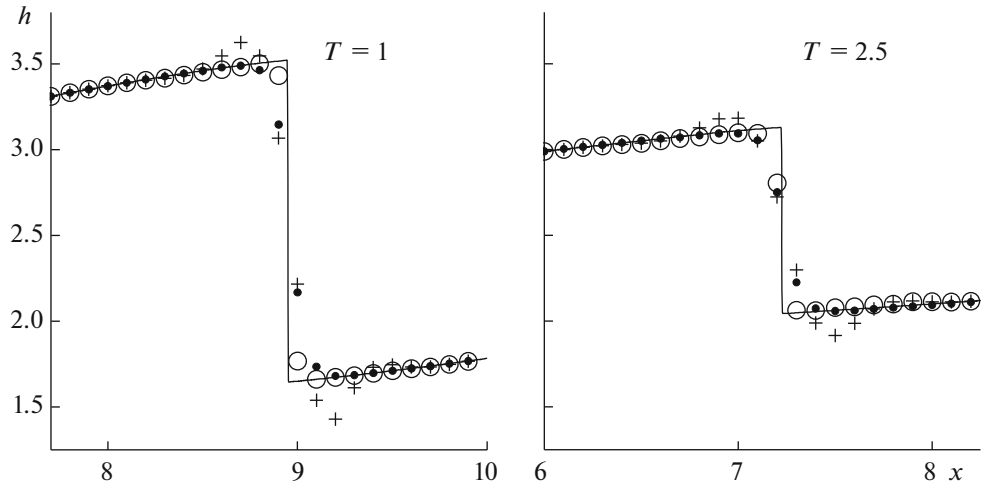

Fig. 2. Fluid depth near the shock front as produced by the combined scheme (open circles), the WENO scheme (solid circles), and Rusanov's scheme (crosses). The solid line depicts the exact solution modeled by the CABARET scheme on a fine grid.

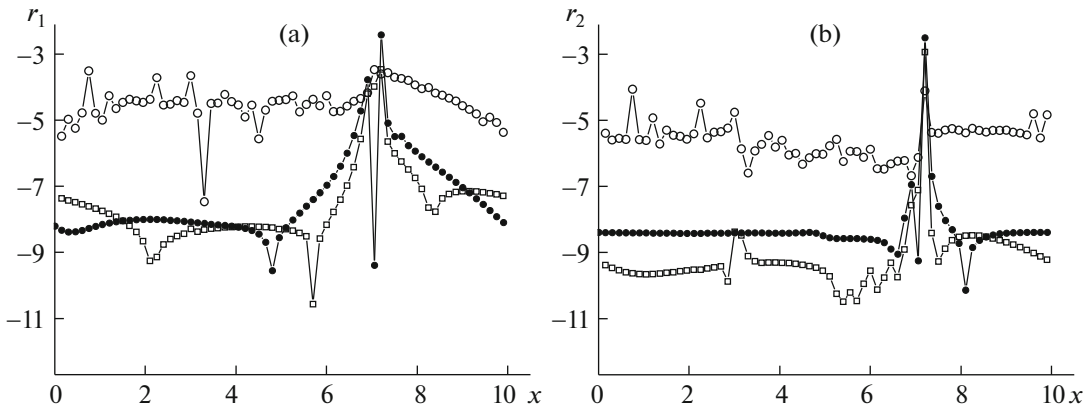

Fig. 3. Grid function $(r_i)_j = \log|\delta w_i(x_j)|$, where $\delta w_i(x_j)$ is the relative local imbalance between the absolute values of the invariants (a) w_1 and (b) w_2 at $T = 2.5$ computed using the present combined scheme (solid circles), the combined scheme from [14] (squares), and the WENO scheme (open circles).

where $\delta w_i(x_j)$ are the relative local imbalances between the absolute values of the invariants (a) w_1 and (b) w_2 computed using the present combined scheme, the combined scheme from [14], and the WENO scheme. The integral orders of convergence and the relative local imbalances were computed by applying the method described in [10, 11] on a basis grid with the spatial stepsize $\Delta = 0.005$, which corresponds to 2000 spatial grid cells on the period-long interval $[0, X]$. The results of these computations are presented for every 20th spatial node $j = 20i$ in Fig. 1 and for every 30th node $j = 30i$ in Fig. 3.

Figure 2 shows that the shock front is localized by the combined scheme monotonically and more accurately than by the WENO scheme. At the same time, Fig. 1 reveals that Rusanov's basis scheme and, hence, the combined scheme based on it, in contrast to the WENO one, preserve the high order of integral convergence on the intervals $[x_j, X]$, whose left endpoints belong to the region of shock influence (this region lies within the interval [4, 9] at the time $T = 1$ and occupies the entire computational domain at $T = 2.5$). This means that the combined scheme transfers the Hugoniot conditions through the shock front with high accuracy, so it preserves the high order of convergence in the region of shock influence. As a result, in the shock influence region, the accuracy of the invariants computed using the combined schemes constructed in this paper and proposed in [14] is higher by several orders of magnitude than that achieved with the WENO scheme (Fig. 3).

ACKNOWLEDGMENTS

This work was supported by the Russian Science Foundation, project no. 16-11-10033.

REFERENCES

1. S. K. Godunov, Mat. Sb. **47** (3), 271–306 (1959).
2. B. Van Leer, J. Comput. Phys. **32** (1), 101–136 (1979).
3. A. Harten, J. Comput. Phys. **49**, 357–393 (1983).
4. H. Nessyahu and E. Tadmor, J. Comput. Phys. **87** (2), 408–463 (1990).
5. G. S. Jiang and C. W. Shu, J. Comput. Phys. **126**, 202–228 (1996).
6. V. M. Goloviznin, M. A. Zaitsev, S. A. Karabasov, and I. A. Korotkin, *New CFD Algorithms for Multiprocessor Computer Systems* (Mosk. Gos. Univ., Moscow, 2013) [in Russian].
7. V. V. Ostapenko, Comput. Math. Math. Phys. **37** (10), 1161–1172 (1997).
8. J. Casper and M. H. Carpenter, SIAM J. Sci. Comput. **19** (1), 813–828 (1998).
9. V. V. Ostapenko, Comput. Math. Math. Phys. **40** (12), 1784–1800 (2000).
10. O. A. Kovyrkina and V. V. Ostapenko, Dokl. Math. **82** (1), 599–603 (2010).
11. O. A. Kovyrkina and V. V. Ostapenko, Math. Models Comput. Simul. **6** (2), 183–191 (2014).
12. N. A. Mikhailov, Math. Models Comput. Simul. **7** (5), 467–474 (2015).
13. V. V. Ostapenko, Comput. Math. Math. Phys. **38** (8), 1299–1311 (1998).
14. O. A. Kovyrkina and V. V. Ostapenko, Dokl. Math. **97** (1), 77–81 (2018).
15. V. V. Rusanov, Dokl. Akad. Nauk SSSR **180** (6), 1303–1305 (1968).

Translated by I. Ruzanova